

University of Wollongong

Research Online

Australian Institute for Innovative Materials -
Papers

Australian Institute for Innovative Materials

1-1-2013

A light-assisted, polymeric water oxidation catalyst that selectively oxidizes seawater with a low onset potential

Jun Chen

University of Wollongong, junc@uow.edu.au

Pawel W. Wagner

University of Wollongong, pawel@uow.edu.au

Lei Tong

University of Wollongong, sbdwtl@gmail.com

Danijel Boskovic

University of Wollongong, db103@uowmail.edu.au

Weimin Zhang

University Of Sydney, University Of Wollongong, weimin@uow.edu.au

See next page for additional authors

Follow this and additional works at: <https://ro.uow.edu.au/aiimpapers>

 Part of the [Engineering Commons](#), and the [Physical Sciences and Mathematics Commons](#)

Research Online is the open access institutional repository for the University of Wollongong. For further information contact the UOW Library: research-pubs@uow.edu.au

A light-assisted, polymeric water oxidation catalyst that selectively oxidizes seawater with a low onset potential

Abstract

Vapour phase polymerisation (vpp) of PEDOT to incorporate high levels of a sulphonated manganese porphyrin yields a vivid green conducting polymer that, under illumination, catalyzes selective oxidation of water from seawater from ca. 0.40 V (vs. NHE; Pt counter electrode) without observable chlorine formation. This onset potential is comparable to that of certain metal oxide semiconductors that achieve higher photocurrents but are not capable of selectively oxidising the water in seawater.

Keywords

onset, polymeric, assisted, light, low, seawater, oxidizes, selectively, that, catalyst, oxidation, potential, water

Disciplines

Engineering | Physical Sciences and Mathematics

Publication Details

Chen, J., Wagner, P. W., Tong, L., Boskovic, D., Zhang, W., Officer, D. L., Wallace, G. G. & Swiegers, G. F. (2013). A light-assisted, polymeric water oxidation catalyst that selectively oxidizes seawater with a low onset potential. *Chemical Science*, 4 (7), 2797-2803.

Authors

Jun Chen, Pawel W. Wagner, Lei Tong, Danijel Boskovic, Weimin Zhang, David L. Officer, Gordon G. Wallace, and Gerhard F. Swiegers

A light-assisted, polymeric water oxidation catalyst that selectively oxidizes seawater with a low onset potential†

Cite this: *Chem. Sci.*, 2013, **4**, 2797

Jun Chen,* Pawel Wagner, Lei Tong, Danijel Boskovic, Weimin Zhang, David Officer, Gordon G. Wallace and Gerhard F. Swiegers*

Received 26th March 2013

Accepted 2nd May 2013

DOI: 10.1039/c3sc50812a

www.rsc.org/chemicalscience

Vapour phase polymerisation (vpp) of PEDOT to incorporate high levels of a sulphonated manganese porphyrin yields a vivid green conducting polymer that, under illumination, catalyzes selective oxidation of water from seawater from ca. 0.40 V (vs. NHE; Pt counter electrode) without observable chlorine formation. This onset potential is comparable to that of certain metal oxide semiconductors that achieve higher photocurrents but are not capable of selectively oxidising the water in seawater.

Introduction

A topic of current interest is the development of efficient light-driven or light-assisted electrodes that facilitate water oxidation catalysis at the most negative possible potentials.^{1–13} The aim is to develop anodes that, when coupled to hydrogen-generating cathodes, can split water at zero bias using light illumination only. Devices of this type have been reported,^{1,2} but are currently commercially unviable because of processing and other features related to the semiconductor substrates. Efforts in this respect have focussed on semiconductors (*e.g.* Si, WO₃, Fe₂O₃ or BiVO₄) with catalysts immobilized on their surface (*e.g.* solid-state Co, Ir or other oxides).^{1–13} Under illumination with sunlight, such electrodes often commence oxygen evolution at onset potentials well below the thermodynamic minimum for the reaction in the dark. Energy from the incident light then drives the catalysis. For example, at pH 7, the thermodynamic minimum for water oxidation without light illumination formally lies at 0.82 V vs. NHE. However, the lowest onset potentials for single junction hybrid devices of the above types typically fall around (Table 1): 0.62–0.75 V (Si),^{1,2} 0.19–0.30 V (BiVO₄, WO₃),^{3–8} 0.29 V (Fe₂O₃, pH 8),^{9–11} and –0.1 V (TaON, pH 8)¹² (vs. NHE; Pt counter electrode). A potential alternative to metal oxide semiconductors is the use of inherently conductive polymers (ICPs) as substrates.

Such polymers are generally more easily processed than metal oxides; for example, as components in flexible devices. Some also display photovoltaic properties when doped with anionic light-harvesting dyes.¹³ Using ICP substrates, it is, moreover, possible to incorporate water oxidation catalysts within the bulk of the semiconductor and not only at its surface. Molecular catalysts can then be used, including putative, “*machine-like*” molecular catalysts. In recent work we demonstrated this concept by showing that poly(terthiophene) doped with a sulphonated Mn porphyrin (**1**) selectively catalyzes light-assisted water oxidation of seawater from 0.91 V vs. NHE, with no Cl₂ produced.¹⁴ Illuminated semiconductors typically yield mixtures of Cl₂ and O₂ in seawater.¹⁵ The catalysis was proposed, but not proven to be carried out by a proportion of the Mn porphyrin monomers which were adventitiously trapped in a noncovalent “*face-to-face*” arrangement capable of repeatedly facilitating bimetallic O₂ formation.¹⁴ Noncovalent *face-to-face* Mn porphyrins have previously been shown to catalyse water oxidation from 0.6 V vs. Ag/AgCl (pH 12).¹⁶ In the current work we report that the more transparent and oxygen-sensitive poly(3,4-ethylene dioxythiophene) (PEDOT), doped with **1** (Scheme 1) during vapour phase polymerisation, is substantially more active as a water oxidation photocatalyst. In seawater it facilitates reaction without notable Cl₂ formation from a remarkably low onset potential of only 0.40 V vs. NHE. This is well below the dark thermodynamic minimum for water oxidation and comparable to the onset potentials of several metal oxide semiconductors. Evidence also exists for extensive formation of noncovalent *face-to-face* porphyrin assemblies in the PEDOT-**1**.

Results and discussion

Semiconductor-based water oxidation catalysis

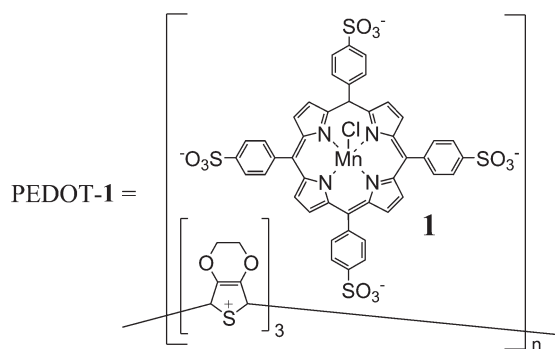
Table 1 tabulates the most negative potentials at which photocurrent is observed (the so-called ‘onset’ potential) for a

Intelligent Polymer Research Institute, ARC Centre of Excellence for Electromaterials Science, University of Wollongong, Wollongong, NSW 2522, Australia. E-mail: junc@uow.edu.au; swiegers@uow.edu.au

† Electronic supplementary information (ESI) available: (1) The preparation of vpp-PEDOT-**1**, (2) its morphological characterisation, (3) the UV-visible measurements, (4) the photocatalytic experiments, (5) 24 h testing data of PEDOT-**1** in seawater, (6) chlorine testing, (7) the electrochemical impedance measurements and their analysis, and (8) how potentials vs. Ag/AgCl were converted into the NHE and RHE scale. The synthesis of the control, chemically polymerised, solution (spray) processed PEDOT-**1** is also described. See DOI: 10.1039/c3sc50812a

Table 1 Reported onset potentials for water oxidation catalysis by selected semiconductors and single-junction semiconductor–catalyst composite anodes. The normal hydrogen electrode (NHE) provides a comparison of the absolute onset potentials; it does not take into account the electrolyte pH ($E_{\text{NHE}} = 0.000$ V). The reversible hydrogen electrode (RHE) provides a comparison that normalises for the pH of the electrolyte ($E_{\text{RHE}} = 0.000 - 0.0591$ (pH))

Semiconductor	Catalyst	pH	Lowest reported onset potentials			Counter electrode	Ref.
			As reported	vs. NHE (V)	vs. RHE (V)		
Si (npp ⁺)	—	7	ca. 1.25 V vs. NHE	1.25	1.66	Pt	1 and 2
	Co–Pi	7	0.60–0.75 V vs. NHE	0.62–0.75	1.03–1.16	Pt	1 and 2
BiVO ₄	—	7	0.0–0.3 V vs. SCE	0.24–0.54	0.65–0.95	Pt	3 and 4
	Co–Pi	7	–0.05 V vs. SCE	0.19	0.60	Pt	3 and 4
	FeOOH	7	0.22 V vs. NHE	0.22	0.63	Pt	5
W:BiVO ₄	—	8	0.60 V vs. NHE	0.60	1.07	Pt	6
	Co–Pi	8	0.30 V vs. NHE	0.30	0.77	Pt	6
SiO ₂ –BiVO ₄	—	7	ca. 0.05 V vs. Ag/AgCl	0.27	0.68	Pt	7
	Co–Pi	7	ca. –0.05 V vs. Ag/AgCl	0.17	0.58	Pt	7
WO ₃	—	7	–0.02 V vs. Ag/AgCl	0.20	0.61	Pt	8a
	Co–Pi	7	–0.2 V vs. Ag/AgCl	0.02	0.43	Pt	8a
CuWO ₄	—	7	–0.05 V vs. Ag/AgCl	0.17	0.58	Pt	8b
Fe ₂ O ₃	—	8	0.37 V vs. Ag/AgCl	0.59	1.06	Pt	9
	Co–Pi	8	0 V vs. Ag/AgCl	0.22	0.69	Pt	9
	Co–Pi	13.6	–0.3 V vs. Ag/AgCl	–0.08	0.72	Pt	9
	Co–Pi	13.6	–0.48 V vs. Ag/AgCl	–0.26	0.54	Pt	10
TaON	—	8	–0.15 V vs. NHE	–0.15	0.32	Pt	11
	CoO _x	8	–0.10 V vs. NHE	–0.10	0.37	Pt	11
ZnO	—	11.5	–0.40 vs. Ag/AgCl	–0.18	0.50	Pt	12
	Co–Pi	11.5	–0.63 vs. Ag/AgCl	–0.41	0.27	Pt	12



Scheme 1

representative selection of previously examined semiconductors and single-junction semiconductor–catalyst combinations. As can be seen, at pH 7, a range of these materials facilitate water oxidation below the dark thermodynamic minimum (0.82 V vs. NHE), down to potentials as low as 0.02 V (vs. NHE) (0.43 V vs. RHE) for Co–Pi on WO₃. In most cases however, an external bias would still be needed to drive the H₂ evolution reaction at the other electrode as the potential range for water oxidation is not negative enough to reduce protons. Nevertheless, the general trend is that surface-immobilization of suitable catalysts (e.g. Co–Pi, CoO_x, or FeOOH) induces the onset potential to shift to more negative potentials, sometimes substantially so. For example, the addition of the Co–Pi catalyst to the surface of the ZnO semiconductor at the bottom of Table 1 moves its onset potential from –0.18 V to –0.41 V vs. NHE at pH 11.5.¹² This was attributed to the Co catalyst decreasing electron–hole recombination at the ZnO surface, thereby shifting the onset potential closer to the ZnO flatband potential, which was found using Mott–Schottky

plots to lie at –0.70 V.¹² Co–Pi/ZnO also gives the lowest onset potential against RHE, which takes into account the pH of the electrolyte (0.27 V vs. RHE).

Inherently conducting polymer–catalyst composites

In recent work we reported that poly(terthiophene) may also yield unusually low, light-assisted onset potentials for water oxidation catalysis when doped with the anionic dye **1**.¹⁴ In that case, catalysis at pH 7 commenced at 0.91 V (vs. NHE; Pt counter electrode), which is only 0.09 V above the thermodynamic minimum potential for the reaction in the dark. The low oxidation potential and the catalytic action allowed for highly selective water oxidation catalysis in seawater. When poised at 1.10 V (vs. NHE; Pt counter electrode) only O₂ and no significant Cl₂, was formed.¹⁴

Poly(terthiophene) was chosen in the earlier study because it is stable over a large electrochemical window within which to facilitate water oxidation catalysis. However, its unusually low onset potential suggested that other conducting polymers, which are stable only at lower potentials, may also be useful as substrates for light-assisted water oxidation. Included amongst these were polypyrrole and PEDOT. PEDOT is more transparent and more conductive than polypyrrole,¹⁷ and also stable to over-oxidation at potentials below ca. 1.00 V (vs. NHE).¹⁷ Accordingly, we studied PEDOT doped with **1** (Scheme 1) as a light-assisted water oxidation catalyst.

Synthesis and characterisation of PEDOT-1 by vapour-phase polymerisation

Films of PEDOT were deposited on ITO glass and ITO-PET sheet using vapour-phase polymerisation,¹⁸ with and without the

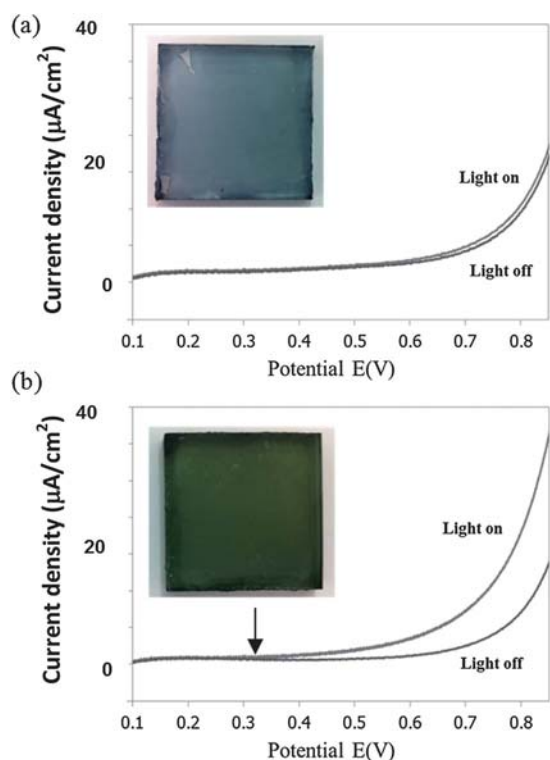


Fig. 1 Current density as a function of potential (vs. Ag/AgCl; scan rate: 5 mV s^{-1}), with and without illumination, of: (a) PEDOT, and (b) PEDOT-1, in aq. 0.1 M Na_2SO_4 (pH 7). The arrow in (b) shows the onset potential for light-assisted water oxidation catalysis. The inset photographs show the visible appearance of the film.

incorporation of the anionic sulfonated Mn-porphyrin **1** (Scheme 1). Without **1**, the PEDOT control films displayed a blue-white appearance (see inset in Fig. 1(a)). However, the PEDOT-1 films had a vivid green coloration (see inset in Fig. 1(b)). UV-visible measurements confirmed the presence of large absorption peaks corresponding to the porphyrin at $\lambda = 350\text{--}450$ nm in PEDOT-1 (Fig. 2). EDX-ray mapping indicated that the porphyrin was uniformly distributed in the PEDOT film

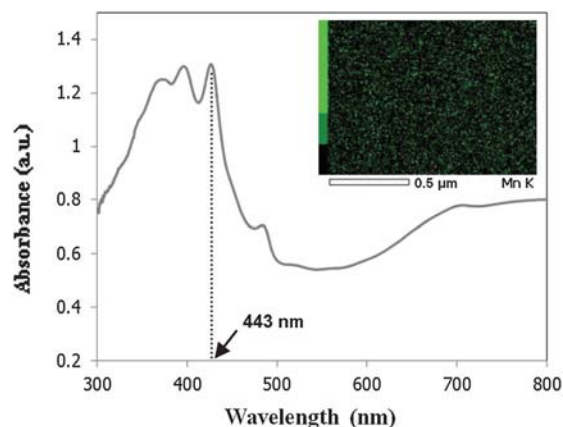


Fig. 2 UV-visible spectrum of PEDOT-1, showing absorption peaks at λ 350–450 nm associated with **1**. The porphyrin Soret band lies at 443 nm. Inset: EDX-ray map of PEDOT-1.

matrix (see inset in Fig. 2). Elemental analysis indicated a mole ratio of 1 Mn porphyrin (identified by Mn) to 3 EDOT monomers (identified by S, normalized to include the S atoms in Mn porphyrin **1**). This is similar to typical doping levels achieved during electrochemical polymerisation of EDOT to form PEDOT films. By this measure, the PEDOT-1 was characterised as containing, on average, three EDOT units for every Mn porphyrin **1** present.

Water oxidation catalysis by PEDOT-1/ITO-glass

For comparative purposes, control films of PEDOT and PEDOT-1 on ITO glass (3 cm^2) were examined as working electrodes in photocatalytic oxygen generation from water. Initial studies were carried out at pH 7 in aqueous 0.1 M Na_2SO_4 electrolyte, with a Pt mesh counter electrode and Ag/AgCl reference electrode. All experiments were carried out under a strict inert atmosphere of either nitrogen or argon. The films were illuminated with a SoLux daylight MR16 halogen light bulb (12 V, 50 W, 24° ; ca. 0.25 sun intensity). The illuminating light was passed through a cut-off filter that blocked all wavelengths above 700 nm to eliminate heating effects.

In order to determine whether a photocurrent was generated, linear sweep voltammograms were carried out at a slow scan rate (5 mV s^{-1}) on the PEDOT and PEDOT-1 films, with and without constant illumination. As can be seen in Fig. 1, PEDOT-1 displays a clear photocurrent commencing from ca. 0.32 V vs. Ag/AgCl (0.55 V vs. NHE). This is substantially below the onset potential for poly(terthiophene)-1 (0.91 V vs. NHE).¹⁴ It is also significantly negative of the theoretical thermodynamic minimum potential for the water oxidation reaction in the absence of illumination (0.82 V vs. NHE).

Studies further examined the use of chopped light during the voltammetric scan, however the rise time of the photocurrent immediately after illumination proved to be relatively long; typically >50 s and up to 200 s to fully establish itself. This is much slower than is common for metal oxide semiconductors of the types discussed earlier and makes it difficult to determine the onset potential using chopped light.

To examine the photocurrent, a PEDOT-1/ITO-glass electrode was studied at a constant potential of 0.70 V vs. Ag/AgCl (0.93 V vs. NHE) in aq. 0.1 M Na_2SO_4 , with and without illumination. Fig. 3 shows the resulting data. As can be seen, a photocurrent develops immediately after illumination, but takes >50 s and up to 200 s to reach its maximum photocurrent. The decline in current after the light is switched off, is somewhat faster. Photocurrents of $>10 \mu\text{A}$ were nonetheless readily achieved.

Oxygen generation by PEDOT-1/ITO-glass

A second experiment involved maintaining the PEDOT-1/ITO-glass electrode (3 cm^2) at a constant potential of 0.6 V vs. Ag/AgCl (0.83 V vs. NHE) whilst subjecting it to more intense illumination of >3 sun provided by a Newport 65902 Xenon lamp. Following extensive purging to remove all ambient O_2 , a constantly flowing inert carrier gas (argon) was maintained through the cell. Prior to illumination, the carrier gas was

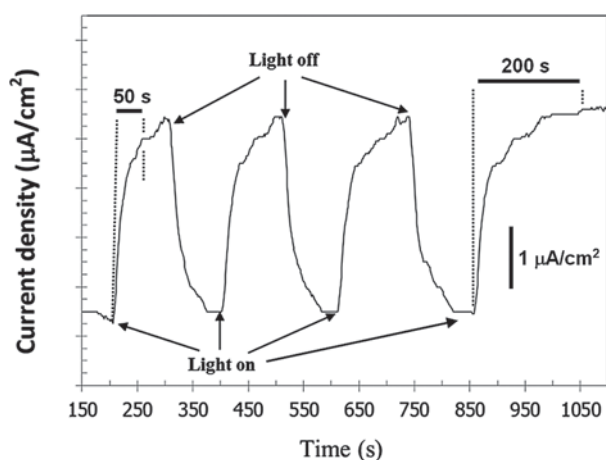


Fig. 3 Photocurrent densities with and without illumination by PEDOT-1/ITO-glass maintained at a constant 0.7 V vs. Ag/AgCl in 0.1 M Na₂SO₄ solution. The points marked "Light on" indicate when the illumination was switched on. The points marked "Light off" indicates when the light was switched off.

sampled using a custom-built gas injection loop connected to a dedicated gas chromatograph. No O₂ was detected. The cell was then illuminated for 1 h (Fig. 4) and the carrier gas sampled again. A clear O₂ response was observed.

Thus, PEDOT-1 unequivocally generates O₂ under illumination even at a potential of 0.83 V (vs. NHE) that is effectively the same as the theoretical thermodynamic minimum for water oxidation in the dark (0.82 V vs. NHE). To the best of our knowledge, this is the first polymeric catalyst that has been shown to facilitate measurable water oxidation at the minimum thermodynamic potential of the reaction.

Current density of PEDOT-1/ITO-glass

The photocurrent data from the above experiment is also of interest. As can be seen in Fig. 4, the photocurrent initially spiked to ca. 90 µA, but then declined to 50 µA. It thereafter increased steadily for the entire period of illumination, up to a

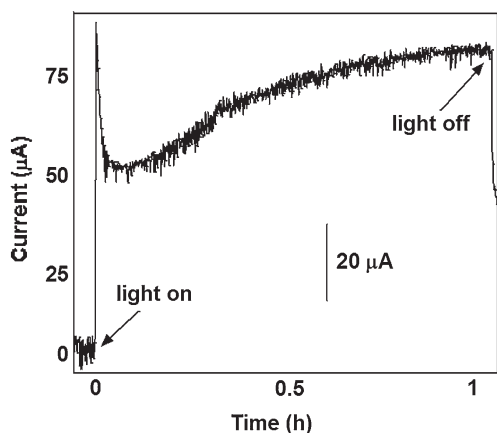


Fig. 4 Photocurrent of a PEDOT-1/ITO-glass electrode in aq. 0.1 M Na₂SO₄ (pH 7) at a potential of 0.60 V vs. Ag/AgCl, under constant illumination with a Newport Oriol 65902 Xenon lamp (>3 sun intensity).

maximum of ca. 78 µA after 1 h, giving the PEDOT-1 a photocurrent density of 26 µA cm⁻². While this is much smaller than the current densities achieved by the earlier-mentioned metal oxide semiconductors, it is, to the best of our knowledge, the largest photocurrent density yet reported for a polymeric water oxidation catalyst below an applied potential of 1 V vs. Ag/AgCl.

Water oxidation catalysis by PEDOT-1/ITO-PET in seawater

Given the unusually low onset potential of PEDOT-1, further studies examined its catalytic performance under illumination in seawater. Metal oxide semiconductors like WO₃ are typically non-catalytic and therefore oxidatively non-selective in electrolytes containing Cl⁻ ions, like seawater.¹⁵ The holes that are formed at the surfaces of such semiconductors are, in effect, sufficiently energetic to extract electrons from either H₂O or Cl⁻. Despite the apparently low applied potentials, Cl₂ may therefore be formed, so that, in electrolytes like seawater, mixtures of O₂ and Cl₂ are usually obtained.

By contrast, we previously found that the catalytic action of poly(terthiophene)-1 under illumination was selective for water oxidation only.¹⁴ It involved an electron shuttle effect, in which light absorption by **1** caused electrons to be transferred from **1** to the poly(terthiophene) matrix. At the externally applied potential, the resulting, neutral form of poly(terthiophene) was necessarily immediately re-oxidized by the electrode back to its conducting form. The remaining oxidized form of **1** must have simultaneously extracted electrons from water. This could potentially have involved a "machine-like" catalytic action in which a tiny proportion of the trapped, oxidized Mn porphyrin monomers repeatedly facilitated bimetallic O₂ formation from two water molecules. Such a mechanism precludes the generation of Cl₂ or HOCl (which equilibrates into Cl₂).

To assess the catalytic performance of PEDOT-1, we repeated the above studies using seawater as the electrolyte. The seawater was collected at Towradgi beach, Wollongong; it displayed a pH of 8.57 and a conductivity of 16.02 mS after filtration.

Fig. 5 depicts linear sweep voltammograms of a flexible 3 cm² PEDOT-1/ITO-PET electrode (shown as the inset in Fig. 5). As can be seen, the onset potential was found to be ca. 0.17 V vs. Ag/AgCl (0.40 V vs. NHE; 0.91 vs. RHE). To the best of our knowledge this is the lowest yet reported onset potential for a polymeric water oxidation catalyst.

Chronoamperograms with and without illumination under different applied potentials were also measured for the same electrode in seawater at 0.60 V, 0.65 V, and 0.70 V vs. Ag/AgCl. The collected data is depicted in Fig. 6. As can be seen, photocurrents of ca. 5, 8, and 17 µA were reproducibly achieved at the above potentials respectively. The time required for the current to rise to its maximum after the commencement of illumination was also shorter (typically >30 s) than was the case at pH 7.

To check for chlorine formation, the experiment at 0.70 V was repeated with constant illumination for 24 h in a sealed cell under inert atmosphere (Fig. S3†). The photocurrent profile was similar to that in Fig. 4, albeit smaller. Gas at the top of the cell and the electrolyte solution itself did not contain Cl₂. Independent measurements using Merckoquant® analytical test

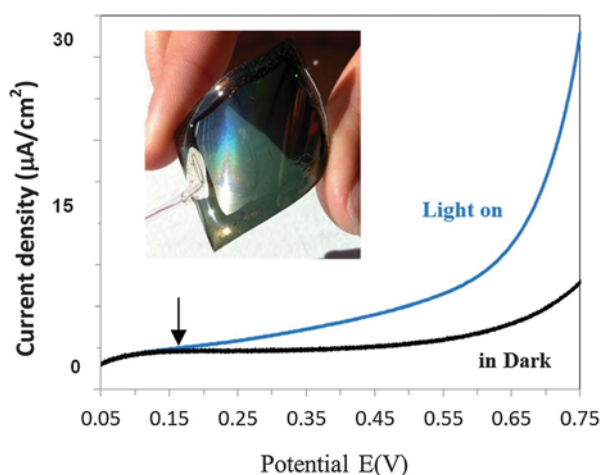


Fig. 5 Current density as a function of potential (vs. Ag/AgCl; scan rate: 5 mV s^{-1}), with and without illumination, of PEDOT-1, in seawater (pH 8.57). The arrow shows the onset potential for light-assisted water oxidation catalysis. The inset photograph shows the visible appearance of the electrode, indicating its flexible nature.

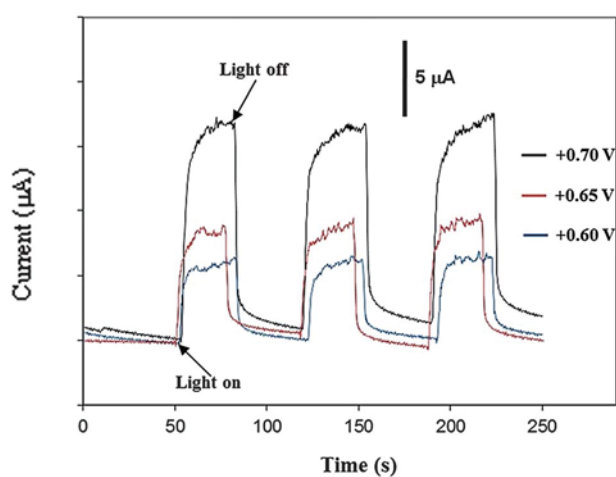


Fig. 6 Current with and without illumination by PEDOT-1/ITO-PET in seawater, at different potentials of +0.60 V, +0.65 V, and +0.70 V (vs. Ag/AgCl; Pt counter electrode). The points marked "Light on" indicate when the illumination was switched on. The points marked "Light off" indicate when the light was switched off. The current profiles have been normalized at the first "light-on" point.

strips indicated an absence of chlorine in the electrolyte after 24 h down to the limit of detection for this technique, which equated to less than 2.3% of the photocurrent going into Cl_2 production (see ESI[†]). By this measure, at least 97.7% of the current went into O_2 formation.

Electrochemical impedance spectroscopy

Water oxidation photocatalysis by PEDOT-1 was also studied using electrochemical impedance spectroscopy (EIS). Fig. 7 shows Nyquist plots of the PEDOT-1 photoanode measured at +0.70 V both in the dark and under illumination. These indicate that the charge transfer resistance of PEDOT-1, related to the big depressed arc at low frequency, dramatically decreases

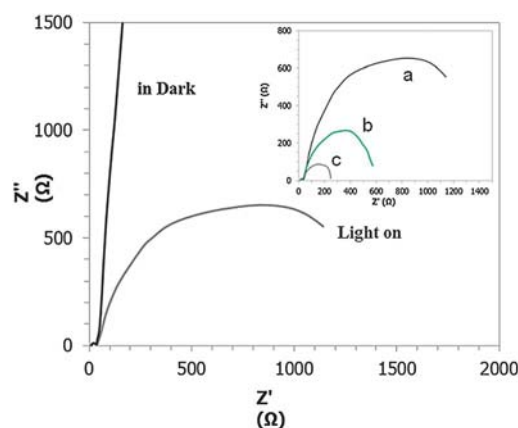


Fig. 7 Electrochemical impedance plots of PEDOT-1/ITO-glass in aq. 0.1 M Na_2SO_4 at 0.70 V vs. Ag/AgCl, with and without illumination, and, within the inset, under illumination at (a) 0.70 V, (b) 0.75 V, and (c) 0.80 V (all vs. Ag/AgCl).

when it is illuminated with light. An equivalent circuit was used to fit the EIS data (Fig. S4[†]). Detailed analysis data are provided in Table S1[†] and clearly indicate that illumination with light facilitates the charge transfer process within the PEDOT-1 electrode. This was confirmed by the decrease in the charge transfer resistance, R_{ct} , under illumination compared with that measured in the dark at +0.7 V. Moreover, increasing the applied potential while under illumination (the inset in Fig. 7) also substantially enhances the catalytic water oxidation, with a smaller depressed arc at successively higher applied potentials that can be attributed to the much lower charge transfer resistance, R_{ct} (shown in Table S1[†]).

"Face-to-face" porphyrin (H-aggregate) formation: the mechanism of catalytic action

A key question that arises out of this work is the mechanism by which photocatalytic water oxidation takes place in PEDOT-1.

In our previous study of poly(terthiophene) doped with 1, we proposed that a tiny proportion of the trapped Mn porphyrins 1 in the electrochemically deposited polymer may be adventitiously arrayed in cofacial "face-to-face" structures capable of repeatedly engaging in bimetallic O_2 formation.¹⁴ Noncovalent face-to-face porphyrin dimers have previously been shown to be water oxidation electrocatalysts at potentials of 0.6 V vs. Ag/AgCl (pH 12).¹⁶ (Monomeric Mn porphyrins are known to be catalytically inactive.)¹⁹ While the evidence was consistent with such an explanation,¹⁴ no direct proof was available to confirm it.

An interesting feature of the present study is that evidence exists for the general formation of noncovalent face-to-face porphyrin dimers within the polymer matrix of vapour-phase polymerised PEDOT-1.

Fig. 2 shows the UV-visible spectrum of vapour-phase polymerised PEDOT-1. As can be seen in Fig. 2, the Soret band of the Mn(III) porphyrin lies at 443 nm.

The UV-visible spectrum of the Mn porphyrin 1 itself (without any PEDOT) is shown in Fig. 8 (broken line). As can be seen, the Soret band lies at 462 nm (Fig. 8).

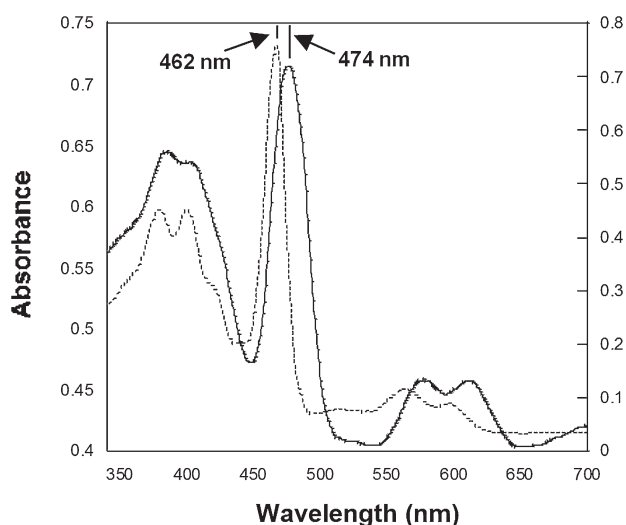


Fig. 8 UV-visible absorption (a.u.) of a thin layer of **1** (broken line; right axis) and solution processed, spray-deposited PEDOT-**1** (solid line; left axis) deposited on a glass slide. As can be seen, the porphyrin Soret band shifts from 462 nm in **1** to 474 nm in the solution-processed, spray-deposited PEDOT-**1**.

Thus, the Soret band in vapour-phase polymerised PEDOT-**1** (443 nm) is significantly blue-shifted relative to the comparable peak in **1** itself (462 nm).

So substantial a blue shift in the Soret band of the vapour-phase polymerised PEDOT-**1** is highly characteristic of the excitonic couplings that occur in *face-to-face* arrayed H-aggregates of porphyrins.²⁰

Moreover, control samples of PEDOT-**1** (containing some PSS for effective dispersion) made by chemical and not vapour-phase polymerisation, and deposited by spray deposition onto a glass slide, display their Soret band at 474 nm (Fig. 8). This is slightly *red-shifted* and not blue-shifted relative to **1** (462 nm).

The chemically polymerised, solution-(spray) processed PEDOT-**1** also displays a negligible photocatalytic effect relative to vapour-phase polymerised vpp-PEDOT-**1**. This is, at least partly because **1** appears to elute from the spray-processed coating after it is immersed in water. No elution of **1** was observed when vpp-PEDOT-**1** was immersed in water.

It therefore appears that, during the vapour phase polymerisation process, the Mn porphyrins **1** in PEDOT-**1** aggregate into particulates containing noncovalent cofacial *face-to-face* species that are trapped within the coating. This is, in fact, reasonably to be expected given that vapour phase polymerisation involves the porphyrins being, first, deposited on the electrode surface with the EDOT monomer then polymerised in the vapour phase above it. That is, during the first step of the polymerisation, high concentrations of the porphyrin are present at the electrode surface, providing ideal conditions for porphyrin aggregation. The aggregates thus formed, are likely locked into place by the PEDOT formed over the top of them.

The resulting vpp-PEDOT-**1** is resistant to porphyrin elution when immersed in water, because the polymer covers the porphyrins and they are, additionally, in aggregates of larger dimensions than the individual porphyrins. Similar conditions

do not exist in the solution- and spray-processed PEDOT-**1**, where the porphyrins appear to be separated and mixed with, rather than covered by the polymer.

The current work differs from our earlier work involving poly(terthiophene) doped with **1**, in that polymerisation was achieved electrochemically in that case and not by vapour-phase polymerisation.¹⁴ The amplification of the catalytic properties in vpp-PEDOT-**1** are therefore implied to arise, at least in part, from the use of vapour-phase polymerisation. In one other previous study, vapour-phase polymerisation was also found to generate a coating with unusually amplified catalytic capabilities.²¹

In summary; the catalytic properties of vpp-PEDOT-**1** appear to derive from the vapour-phase polymerisation technique used and, specifically, from the aggregation of the porphyrins **1** in noncovalent cofacial *face-to-face* arrays that occurs during that process. These aggregations must, at present, be considered to be the key sites of catalytic activity, since similar structures are known to be catalytic in water oxidation.¹⁶

The mechanism of light-assisted catalysis in PEDOT-**1** is likely similar to that identified in the previous study involving poly(terthiophene),¹⁴ namely, light absorption by **1**, followed by electron injection from **1** into the PEDOT matrix. At the applied voltage, the resulting reduced form of PEDOT would be immediately oxidized by the electrode, creating charge separation. The remaining 1^+ would then be ideally set up to interact with an adjacent, cofacial *face-to-face* Mn porphyrin in its assembly and thereby extract electrons from two reactant water molecules to generate dioxygen.

Conclusions

This work has examined vapour-phase polymerised (vpp) PEDOT-**1** as a polymeric water oxidation photocatalyst. We have shown that vpp-PEDOT-**1** catalyses oxygen generation from water with the lowest onset potential and largest current density yet reported for a polymeric catalyst at pH 7–9 and an applied bias below 1.00 V *vs.* Ag/AgCl. Unlike many metal oxide semiconductors, vpp-PEDOT-**1** appears to selectively oxidize the water reactant in seawater, producing only dioxygen with no measurable chlorine generated. While the photocurrents produced by PEDOT-**1** are orders of magnitude smaller than those generated by conventional metal oxide semiconductors, they are notable. They are also relatively stable during testing over periods of hours. Vapour phase polymerised PEDOT-**1** moreover, appears to contain large proportions of noncovalent cofacial Mn porphyrins in *face-to-face* arrangements. Assemblies of similar type have previously been shown to be electrocatalysts of water oxidation.

Acknowledgements

The authors thank Dr Attila Mozer for helpful discussions. This work was supported by the Australian Research Council Grant number CE0561616, The Australian Centre of Excellence for Electromaterials Science.

Notes and references

- 1 D. G. Nocera, *Acc. Chem. Res.*, 2012, **45**, 767, and refs therein.
- 2 J. J. H. Pipers, M. T. Winkler, Y. Surendranath, T. Buonassisi and D. G. Nocera, *Proc. Natl. Acad. Sci. U. S. A.*, 2011, **108**, 10056.
- 3 D. Wang, R. Li, J. Zhu, J. Shi, J. Han, H. Zong and C. Li, *J. Phys. Chem. C*, 2012, **116**, 5082.
- 4 T. H. Jeon, W. Choi and H. Park, *Phys. Chem. Chem. Phys.*, 2011, **13**, 21392.
- 5 J. A. Seabold and K.-S. Choi, *J. Am. Chem. Soc.*, 2012, **134**, 2186.
- 6 D. K. Zhong, S. Choi and D. R. Gamelin, *J. Am. Chem. Soc.*, 2011, **133**, 18370.
- 7 S. K. Pilli, T. G. Deutsch, T. E. Furtak, J. A. Turner, L. D. Brown and A. M. Herring, *Phys. Chem. Chem. Phys.*, 2012, **14**, 7032.
- 8 (a) J. A. Seabold and K.-S. Choi, *Chem. Mater.*, 2011, **23**, 1105; (b) J. E. Yourey and B. M. Bartlett, *J. Mater. Chem.*, 2011, **21**, 7651; J. E. Yourey, J. B. Kurtz and B. M. Bartlett, *J. Phys. Chem. C*, 2012, **116**, 3200.
- 9 D. K. Zhong and D. R. Gamelin, *J. Am. Chem. Soc.*, 2010, **132**, 4202.
- 10 Y.-R. Hong, Z. Liu, S. Fatanah, B. S. A. Al-Bukhari, C. J. J. Lee, D. L. Yung, D. Chi and T. S. A. Hor, *Chem. Commun.*, 2011, **47**, 10653.
- 11 M. Higashi, K. Domen and R. Abe, *J. Am. Chem. Soc.*, 2012, **134**, 6968, and refs therein.
- 12 E. M. P. Steinhilber and K.-S. Choi, *Proc. Natl. Acad. Sci. U. S. A.*, 2009, **106**, 20633.
- 13 See for example: G. Tsekouras, C. O. Too and G. G. Wallace, *Synth. Met.*, 2007, **157**, 441.
- 14 J. Chen, P. Wagner, G. F. Swiegers, D. L. Officer and G. G. Wallace, *Angew. Chem., Int. Ed.*, 2012, **51**, 1907.
- 15 See for example: J. C. Hill and K.-S. Choi, *J. Phys. Chem. C*, 2012, **116**, 7612; B. D. Alexander and J. Augustynski, Chapter 12. Nanostructured Thin-Film WO₃ Photoanodes for Solar Water and Sea-Water Splitting, in *On Solar Hydrogen and Nanotechnology*, ed. L. Vayssieres, Wiley, Singapore, 2009.
- 16 L. Ruhlmann, A. Nakamura, J. G. Vos and J.-H. Fuhrop, *Inorg. Chem.*, 1998, **37**, 6052.
- 17 (a) A. Kros, S. W. F. M. Van Hovell, N. A. J. M. Sommerdijk and R. J. M. Nolte, *Adv. Mater.*, 2001, **13**, 1555; (b) A. Kros, R. J. M. Nolte and N. A. J. M. Sommerdijk, *Adv. Mater.*, 2002, **14**, 1779; (c) A. Kros, N. A. J. M. Sommerdijk and R. J. M. Nolte, *Sens. Actuators, B*, 2005, **106**, 289.
- 18 B. Winther-Jensen, J. Chen, K. West and G. G. Wallace, *Macromolecules*, 2004, **37**, 5930; J. Chen, B. Winther-Jensen, C. Lynam, O. Nagmna, S. Moulton and G. G. Wallace, *Electrochem. Solid-State Lett.*, 2006, **9**, H68.
- 19 Y. Naruta, M. Sasayama and T. Sasaki, *Angew. Chem., Int. Ed. Engl.*, 1994, **33**, 1839.
- 20 A. Satake and Y. Kobuke, *Org. Biomol. Chem.*, 2007, **5**, 1679.
- 21 For an earlier example of vapour-phase polymerisation yielding unusual catalytic properties, see: J. Chen, W. Zhang, D. Officer, G. F. Swiegers and G. G. Wallace, *Chem. Commun.*, 2007, 3353.